
ECM: A Unified Electronic Circuit Model for Explaining the Emergence of In-Context Learning and Chain-of-Thought in Large Language Model

Qiguang Chen[†] Libo Qin^{‡*} Jinhao Liu[†] Dengyun Peng[†] Jiaqi Wang[◇]

Mengkang Hu[♣] Zhi Chen[♠] Wanxiang Che^{†*} Ting Liu[†]

[†] Research Center for Social Computing and Information Retrieval

[†] Harbin Institute of Technology

[‡] School of Computer Science and Engineering, Central South University

[◇] The Chinese University of Hong Kong

[♣] The University of Hong Kong

[♠] ByteDance Seed (China)

{qgchen, car}@ir.hit.edu.cn, lbqin@csu.edu.cn

Abstract

Recent advancements in large language models (LLMs) have led to significant successes across various applications, where the most noticeable is to a series of emerging capabilities, particularly in the areas of In-Context Learning (ICL) and Chain-of-Thought (CoT). To better understand and control model performance, many studies have begun investigating the underlying causes of these phenomena and their impact on task outcomes. However, existing explanatory frameworks predominantly focus on isolating and explaining ICL and CoT independently, leading to an incomplete understanding of their combined influence on model performance. To address this gap, we propose the Electronic Circuit Model (ECM), which provides a foundation for developing scalable, learnable policies and improving the management of AI-generated content. Specifically, ECM conceptualizes model behavior as an electronic circuit: ICL is represented as semantic magnetic field to providing an additional voltage following Faraday’s Law, while CoT is modeled as series resistors to constrain the model output performance following Ohm’s Law. Experimental results demonstrate that the ECM effectively predicts and explains LLM performance across a variety of prompting strategies. Furthermore, we apply ECM to advanced reasoning strategy optimization on a series of tasks, such as the International Olympiad in Informatics (IOI) and the International Mathematical Olympiad (IMO), achieving competitive performance that surpasses nearly 80% of top human competitors.

Key Words: Electronic Circuit Model, Large Language Model, In-Context Learning, Chain-of-Thought

1 Introduction

Large Language Models (LLMs) have made significant strides across various tasks, including code generation, knowledge-based question answering, and complex reasoning [46, 3, 29, 32]. Unlike earlier models that showed incremental improvements, LLMs exhibit emergent capabilities that fundamentally reshape problem-solving. At the core of these capabilities are two critical mechanisms: In-Context Learning (ICL) [2, 11, 31] and chain-of-Thought (CoT) reasoning [26, 41, 5],

*Corresponding Author

enabling LLMs to adapt dynamically to new challenges and achieve human-comparable learning and reasoning [2, 27, 1]. Specifically, ICL triggers LLMs to generalize information based on task-specific context provided in the input, without requiring parameter updates. In parallel, CoT reasoning allows LLMs to approach complex problems stepwise, enhancing both performance and interpretability. Together, these mechanisms empower LLMs to serve as versatile problem solvers in critical fields such as healthcare and education [14, 25, 16, 18].

Despite their transformative potential, the mechanism of LLMs’ emergent capabilities remains poorly understood. Current research on ICL has uncovered preliminary evidence of how models encode and process contextual information, with studies suggesting latent representations that approximate forms of task-specific meta-learning [38, 36] or topic models [39]. Similarly, CoT research has begun to map the reasoning pathways LLMs employ, providing insights into their demonstration alignment with human cognitive heuristics [24, 37]. Others seek to interpret emergent behaviors using macroscopic mathematical models based on experimental analysis [13, 5]. In practice, ICL and CoT are often integrated, allowing models to adapt to context and solve problems step-by-step [17, 15, 30, 47, 6]. To put it figuratively, combining ICL and CoT is like planting a tree: ICL provides the rich “soil” in which the model can absorb and integrate contextual knowledge, while CoT guides its “branches” to grow step by step in a clear, structured direction. Together, they create a natural, human-like reasoning process that’s both flexible and transparent, enabling models to tackle complex tasks with greater depth and precision. Unfortunately, in the current literature, a unified understanding of the combined effect of ICL and CoT remains limited, which seriously affects correct performance interpretation and controllable result prediction and further constrains the development of principled methodologies for LLM design and deployment.

To bridge this gap, we introduce the Electronic Circuit model (ECM), a unified theoretical paradigm that reimagines model performance through the lens of physical circuit systems. Specifically, as shown in Figure 1, we try to conceptualize ICL capabilities as semantic magnetic fields, driving additional voltage gains that correspond to enhanced information absorption, while CoT challenges are modeled as series resistors, introducing predictable constraints akin to circuit losses. Based on these hypotheses, we discover Faraday’s Law of ICL and Ohm’s Law of CoT in LLMs’ reasoning process. By rigorously aligning theoretical circuit power predictions with empirical accuracy results across 3 prompting strategies, 4 task categories, and 13 different LLMs. The ECM successfully establishes a unified quantitative paradigm for predicting and optimizing the behavior of LLMs.

Moreover, based on the introduction of ECM, we further explain over 10 existing prompt optimization strategies from the perspective of optimizing the magnetic field and optimizing the resistors. And given these perspectives, some phenomena that have not been successfully explained by previous works and more excellent prompt strategies are discovered based on ECM. Notably, our results show that combined with these approaches has achieved breakthroughs in complex domains: LLMs guided by ECM-optimized strategies have outperformed over 80% of human competitors in the International Olympiad in Informatics and the International Mathematical Olympiad. Furthermore, in subjective and exploratory contexts such as academic research development, ECM-optimized strategies have driven significant gains, achieving a minimum 10% improvement in overall human scores.

In summary, our contributions are as follows:

- To the best of our knowledge, we are taking the first meaningful step to introduce the Electronic Circuit Model (ECM), effectively offering a unified theoretical paradigm to reformulate model performance through the lens of circuit systems.
- In this framework, we discover Faraday’s Law of ICL and Ohm’s Law of CoT in LLMs’ reasoning, and further utilize ECM to effectively predict the empirical accuracy and explain the effectiveness of 10 existing strategies from the view of optimizing the magnetic field and optimizing the resistor.
- We utilize ECM to explain some open phenomena and to propose more excellent prompt strategies based on ECM. Combined with these approaches, we have achieved breakthroughs in mathematical and code competition and academic research development scenarios. Further, we empirically demonstrate that applying ECM-driven optimizations to LLMs leads to substantial performance gains.

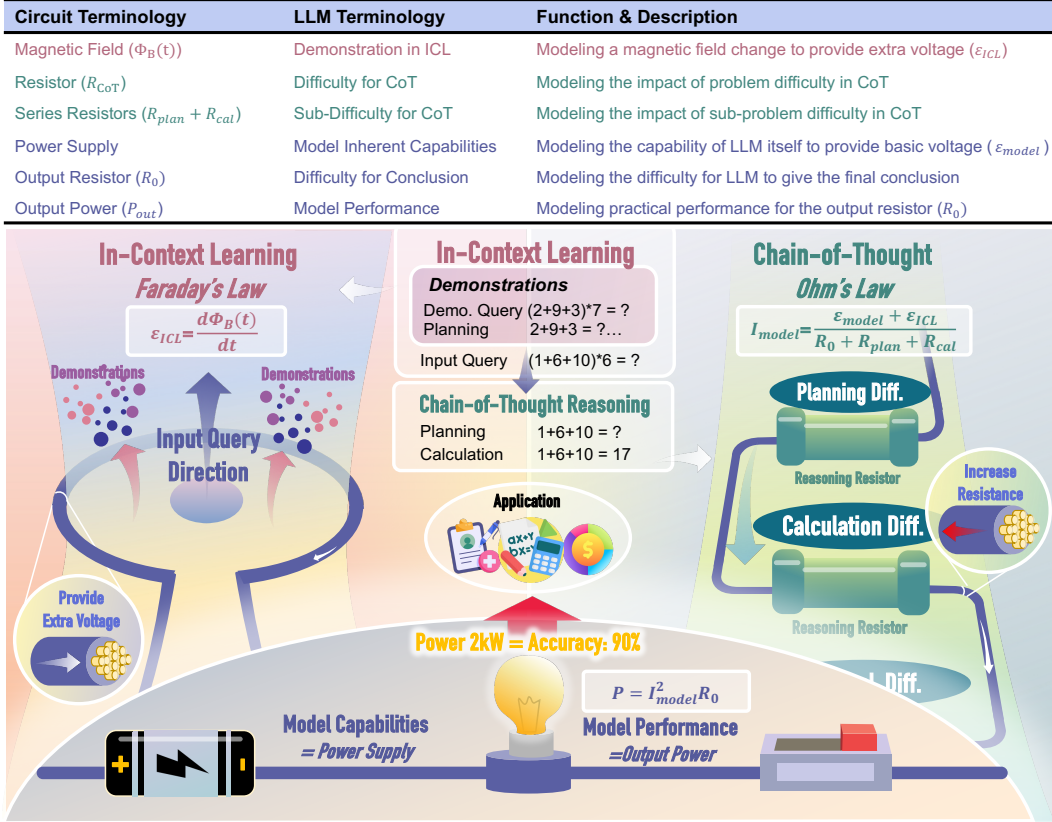


Figure 1: **Glossary of Terms and Schematic of Electronic Circuit Model (ECM).**

In-Context Learning (ICL) is conceptualized as a (Semantic) Magnetic Field. Demonstrations in ICL effectively provide an additional voltage by applying a magnetic field change aligned with the input query direction. Chain-of-Thought (CoT) process is analogized as series resistors in circuit, where the reasoning difficulty in CoT are divided into a sequence of sub-difficulties, analogous to resistors in a circuit that collectively increase overall resistor. Building on this, we introduce the concept of model inherent capabilities, represented as the power supply of the circuit to provide basic voltage. Model performance can then be quantified as the circuit’s output power, enabling more precise predictions of empirical accuracy. In addition, in this article, “strength” denotes the value of semantic magnetic fields, “resistance” denotes the value of resistor, and “voltage” denotes the value of power supply.

2 Theoretical Model

This theoretical model shows that model performance (P_{out}) relies not only on basic voltage from model inherent capabilities (ϵ_{model}) but also on external factors like reasoning difficulty (R_{CoT}) and additional voltage from extra demonstrations in ICL (ϵ_{ICL}), which are described as follows in detail:

2.1 Model Inherent Capabilities as Power Supply

In our model, we draw an analogy by conceptualizing LLM’s inherent capabilities as a power supply that drives computational processes and reasoning tasks (Figure 1). The voltage value ϵ_{model} represents the strength of the inherent capability, governing the LLM’s capacity to execute a range of tasks. Just as the voltage in an electrical circuit determines the power available to drive various components, the internal capabilities govern its ability to manage increasingly complex inputs.

2.2 Faraday’s Law of In-Context Learning

Inspired by Wang et al. [38], the process of ICL can be conceptualized as the interaction of LLM with contextual data, where it absorbs, retains, and eventually releases semantic information flow.

This dynamic flow of information resembles the changing behavior of a magnetic field as its initial strength Φ_0^B decreases to zero. Building on this analogy, we propose Faraday’s Law for the ICL paradigm, where the rate of change in the “magnetic field” further induces an extra voltage:

$$\mathcal{E}_{\text{ICL}} = -\frac{d\Phi^B(t)}{dt} = \lambda\Phi_0^B, \quad (1)$$

where λ represents the uniform rate of decrease in magnetic field intensity. This perspective enables a deeper quantitative understanding of ICL through the concept of a “semantic magnetic field,” as illustrated in Figure 1.

2.3 Ohm’s Law of Chain-of-Thought

In a parallel vein, Chen et al. [5] have discovered a combination law for LLM reasoning, which aligns with the series formula of electrical resistors after transformation (See in Appendix A). Inspired by this, we conceptualize the difficulty of CoT reasoning as analogous to series circuits. In this framework, each reasoning process introduces a distinct resistor ($R_{\text{CoT}} = \sum_i R_i$), compounding the task’s overall difficulty (R_i). As illustrated in the right panel of Figure 1, Ohm’s law for CoT can be expressed as:

$$I_{\text{model}} = \frac{\mathcal{E}_{\text{model}} + \mathcal{E}_{\text{ICL}}}{R_{\text{CoT}} + R_0}, \quad (2)$$

where R_0 represents the resistance of an output resistor with static resistance value in the circuit, which reflects the difficulty of reasoning conclusion. This formulation quantifies the cumulative effect of reasoning resistors, providing a modular quantitative perspective on cognitive task complexity.

2.4 Model Performance as Output Power of Bulb

Extending the conceptual model, we equate model performance to the power output of a light bulb in an electronic circuit. Task execution efficiency depends on a nonlinear interaction of internal and external factors, rather than solely on the model’s intrinsic capabilities. The output power, P_{out} , is expressed as:

$$P_{\text{out}} = I_{\text{model}}^2 R_0 = \frac{(\mathcal{E}_{\text{model}} + \mathcal{E}_{\text{ICL}})^2 R_0}{(R_{\text{CoT}} + R_0)^2}. \quad (3)$$

Here, output power represents the model’s effective performance, with higher power indicating better task execution, akin to a brighter bulb. The equation highlights that maximizing performance requires enhancing the basic voltage of power supply ($\mathcal{E}_{\text{model}}$) of LLM, minimizing reasoning resistor (R_{CoT}) in CoT, and optimizing the extra voltage (\mathcal{E}_{ICL}) provided by ICL. This synergy explains and predicts the model’s performance on complex tasks quantitatively.

3 Theoretical Model Verification

3.1 CoT Meets Ohm’s Law

First, we verify whether CoT adheres to Ohm’s law. Since the electric current I_{model} in Eq. 2 is not directly observable, we instead examine whether P_{out} is linearly related to true accuracy, thereby indirectly validating CoT Ohm’s law. Specifically, to control variables, we remove the ICL and let the model perform zero-shot reasoning step-by-step following the instructions, which satisfies: $P_{\text{out}} = \frac{\mathcal{E}_{\text{model}}^2 R_0}{(R_{\text{CoT}} + R_0)^2}$. The strong Spearman correlation coefficient between theoretical power (P_{out}) and observed accuracy (Acc), shown in Figure 2a, is 0.8843, with a p -value below 0.01. This strong correlation suggests difficulty of CoT reasoning actually exhibits resistor-like behavior, making it a reliable predictor of model performance.

3.2 ICL Meets Faraday’s Law

We conceptualize contextual demonstrations in ICL as a semantic magnetic field governed by Faraday’s Law during reasoning. Under this framework, semantic influence and proximity are quantified by projection length, as illustrated in the lower right of Figure 2b. To validate this hypothesis, we evaluate various metrics for contextual proximity between demonstrations and user

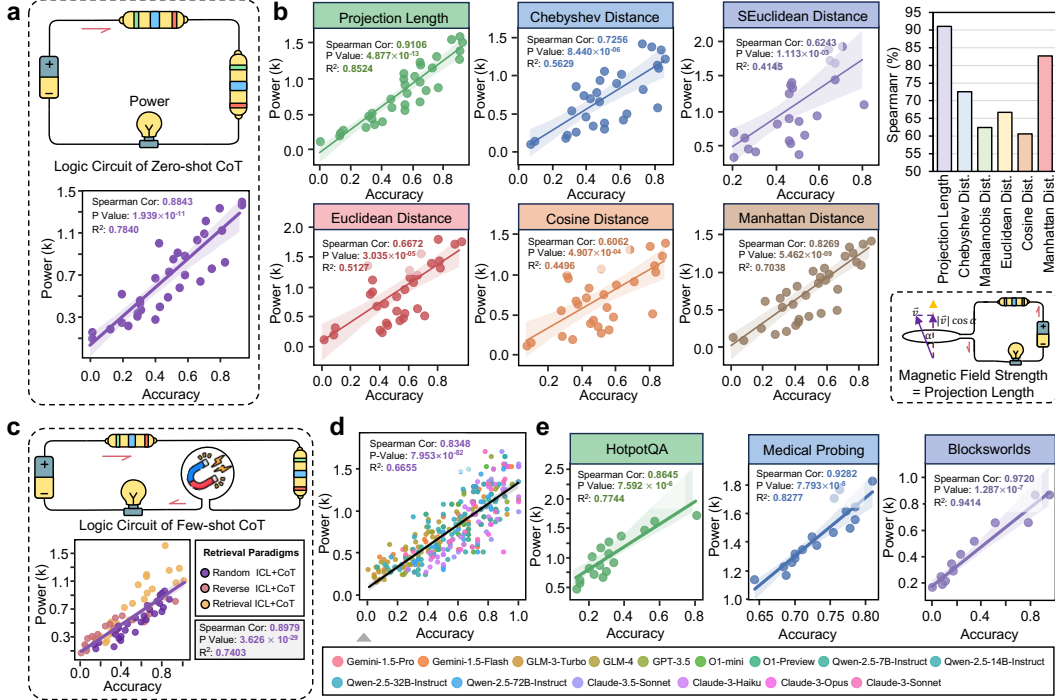


Figure 2: **The Experimental Results of Theoretical Model Verification on ECM.**

a, An analysis of ECM incorporating the CoT approach reveals a scatter plot illustrating the relationship between model accuracy and theoretical power with 0.8843 Spearman coefficient. **b**, Six similarity metrics are employed to evaluate whether context demonstrations can be interpreted as a semantic magnetic field. The results indicate that the projection length achieving the highest coefficient of 0.9106 between practical accuracy and theoretical power. **c**, The integrated ECM framework combines ICL and CoT. Across three retrieval strategies for ICL demonstrations, a consistent linear correlation is observed. **d**, Experiments on various LLMs under different power supply voltages, representing their capacities, reveal a strong linear correlation between theoretical power estimates and observed accuracy. **e**, Broader analyses across diverse tasks, including multi-hop knowledge reasoning, medical probing, and robotic planning, demonstrated robustness.

requests. Our analysis (Figure 2b) shows that the Spearman correlation between the calculated power P_{model} in Eq. 3 and observed spearman coefficient and R^2 merely for projection length exceeds 0.85. This indicates that the geometric alignment of the demonstrations with the task request is a strong predictor of model performance, which further prove the existence of Faraday’s Law of ICL.

3.3 ICL and CoT Satisfy a Unified ECM

In an unprecedented integration, we unify ICL and CoT within a single ECM, offering a comprehensive framework to explain their interaction and collective impact on model performance. We rigorously test this unified model using three distinct retrieval strategies for ICL demonstrations, all of which yields a consistent linear distribution, as illustrated in Figure 2c. This consistent alignment, with a Spearman correlation coefficient of 0.8979 and a p -value approaching zero between calculated power in Eq. 3 and practical accuracy, provides strong empirical evidence for the robustness of our theoretical model. These results confirm that both ICL and CoT not only can be calculated independently but are inherently compatible within the same theoretical structure, offering a powerful new way to describe and predict the behavior of LLM systems.

3.4 Extension Experiments on Various LLMs and Tasks.

To demonstrate the generality of our theoretical ECM, we conduct extension experiments across LLMs configured with varying power supply voltages to represent different capacities. Figure 2d reveals a consistent linear correlation over 0.8348 between theoretical output power estimates and empirical accuracy, confirming the ECM’s robustness in predicting performance. Beyond traditional

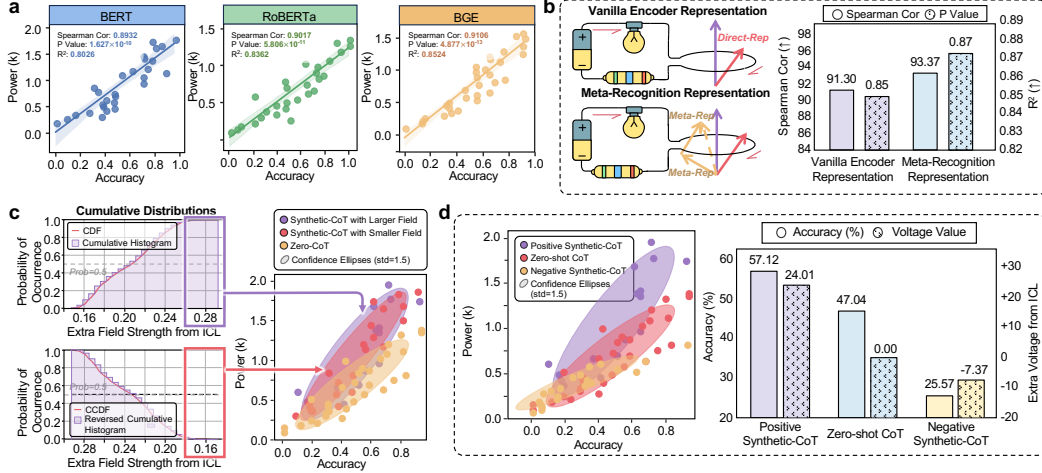


Figure 3: **The Experimental Explanation for Existing ICL Strategies.**

a, The relationship between theoretical power and actual accuracy for various encoders is assessed. BGE achieves the highest Spearman correlation coefficient of 0.9106. **b**, A comparison of the Vanilla Encoder and the Meta-Recognition Representation reveals the latter’s ability to enhance the linear correlation between theoretical power and practical accuracy, from 0.9130 to 0.9337. **c**, The distribution of magnetic field strengths in generated demonstrations (with CDF representing cumulative distribution function and CCDF representing complementary cumulative distribution function). Further, we demonstrates the effectiveness of different Synthetic-CoT with degree of different degree of semantic field strength. **d**, The effectiveness of Synthetic-CoT is analyzed across three conditions: Positive Synthetic-CoT (demonstrations with positive extra voltage from ICL based on positive magnetic fields), Zero-shot CoT (no demonstrations), and Negative Synthetic-CoT (demonstrations with negative extra voltage from ICL based on negative magnetic fields). The left scatter plot displays the performance distribution of these conditions on the power-accuracy landscape. The right bar chart highlights factors contributing to Synthetic-CoT’s optimization of extra voltage provided by ICL.

mathematical reasoning tasks, we test ECM on diverse real-world problems, including multi-hop knowledge reasoning [44], medical probing [7], and robotic planning [34]. As shown in Figure 2e, ECM achieves Spearman coefficients exceeding 0.86 and R² exceeding 0.77 across all tasks, underscoring its versatility in both cognitive and practical applications.

4 Explanation based on ECM

In this section, we mainly pay attention to how to use ECM to explain the effectiveness of existing prompting methods.

4.1 Explanation for ICL Strategies

Enhanced embeddings facilitate accurate semantic magnetic field strength estimation and retrieval. Recent advancements in embedding models have shown that improved text representations directly enhance LLM’s efficacy in the retrieval process [21]. This improvement is tied to the precise estimation of semantic magnetic field strength. As shown in Figure 3a, we employ three models—BERT [9], RoBERTa [22], and BGE [4]—to represent and retrieve demonstrations in ICL. Among these, BGE achieves the highest degree of alignment, with a Spearman correlation coefficient of 0.9106 between theoretical power and empirical accuracy, significantly surpassing the other models. This result highlights superior embedding ability attributed to the accurate semantic magnetic field estimation.

Meta Recognition Enhance Magnetic Field Strength Estimation Modeling. The study of Dildolkar et al. [10] introduces Meta-Recognition, a method leveraging GPT-4 [1] to decompose complex problems into modular sub-capabilities for ICL representation, improving LLMs’ performance. We at-

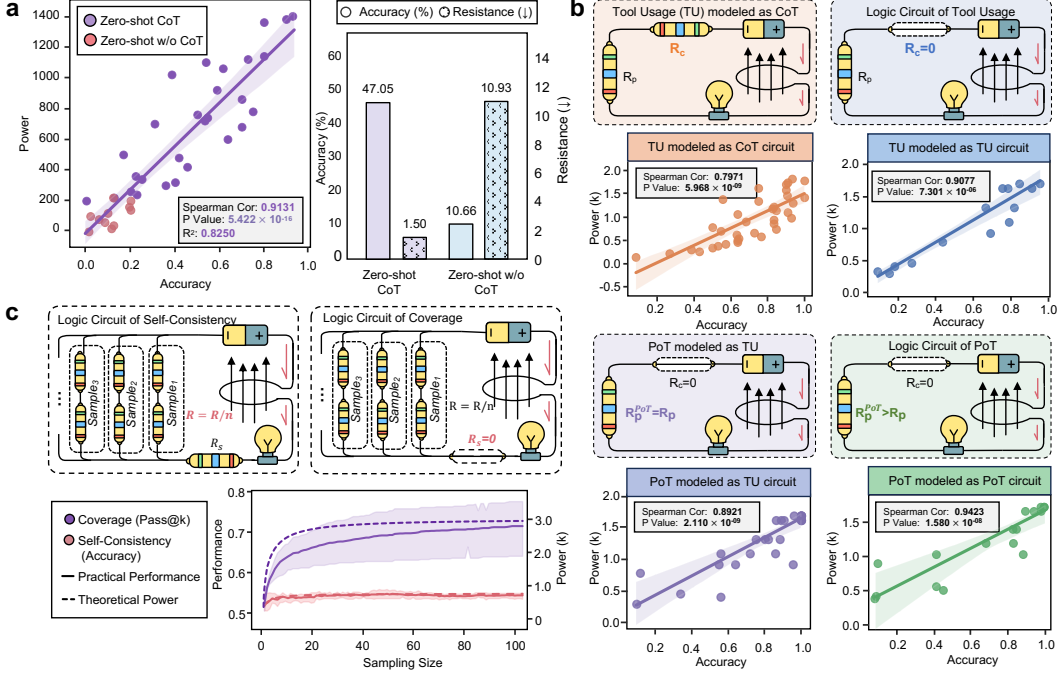


Figure 4: **The Experimental Explanation for Existing CoT Strategies.**

a, The distributions of accuracy, power, and resistance for Zero-shot without CoT and Zero-shot with CoT are presented. The average resistance for Zero-shot without CoT is 10.93, significantly higher than the 1.50 observed for Zero-shot with CoT. **b**, Mechanistic analysis of Tool Usage (TU) and Program-of-Thought (PoT) within the ECM. Initially, TU, modeled on the original CoT, had non-zero computational resistance (R_C), limiting power-accuracy correlation. Assuming $R_C = 0$ achieves a 10% improvement in the Spearman coefficient. PoT, representing TU with structured code, further enhanced performance by keeping $R_C = 0$ and reducing planning resistance R_P , achieving another 10% improvement in power-accuracy correlation. **c**, A circuit-based rationale to explain how to utilize self-consistency and coverage to enhance performance. Self-consistency reduces total resistance by processing multiple reasoning resistors in parallel (sampling n solutions and selecting the output with the highest consensus). In contrast, coverage minimizes resistance by increasing sample size with negligible resistance of voting resistor (sampling n instances and passing the task if any succeeds).

tribute its effectiveness to the enhanced sample representation modeling, which enhances ICL voltage and subsequently boosts output power and accuracy. As illustrated in Figure 3b, Meta-Recognition significantly increases the correlation between theoretical power and practical accuracy, improving from 0.9130 to 0.9337. It underscores that representation based on sub-capability decomposition effectively enhances the precision of magnetic field strength modeling.

Synthetic-CoT predominantly generates samples with positive magnetic fields, enhancing model performance. Synthetic-CoT, a widely used approach in ICL, enables LLMs to autonomously generate ICL demonstrations, thereby improving performance [33]. As illustrated in Figure 3d, all ICL demonstrations produced by Synthetic-CoT exhibit positive semantic magnetic field contributions, which are strongly correlated with enhanced model accuracy. This effect is likely due to the positive voltage induced by the magnetic field, which optimizes circuit functionality. As shown in Figure 3d, the larger ICL magnetic field strength corresponds to the larger power and the higher accuracy. To further investigate the impact of magnetic field polarity on model performance, we analyzed demonstrations with negative magnetic field. Including such examples led to a 21.47% reduction in accuracy and a substantial decline in theoretical power output (Figure 3d). These findings underscore the critical role of positive magnetic field demonstrations in the superior performance achieved by Synthetic-CoT.

4.2 Explanation for CoT Strategies

Direct Answering Introduces Greater Logical Resistor Compared to CoT Recent studies suggest that generating direct answers without intermediary reasoning steps increases cognitive load on the model [13, 17]. We hypothesize that the absence of explicit reasoning pathways introduces significant resistance of “logical resistor,” leading to weaker performance compared to Zero-shot CoT. To test this, we analyzed performance and power correlations for direct answering and Zero-shot CoT on a power-accuracy graph, finding a strong linear correlation of 0.9131 (p -value < 0.01). The average resistance for direct answering is calculated as 10.93, substantially higher than the 1.50 observed for Zero-shot CoT. This discrepancy corresponds to a performance reduction of over 30% for direct answering. These findings indicate that the lack of a CoT framework imposes additional greater logical resistor, hindering the model’s reasoning capabilities and resulting in diminished performance.

Tool Usage optimizes computational resistor, and PoT further reduces planning resistor, improving model performance. Chen et al. [5] propose that Program of Thought (PoT) and Tool Usage (TU) enhance computational reasoning capabilities to a theoretical maximum, effectively minimizing reasoning complexity to zero, akin to eliminating the resistance to zero. Inspired by this, we investigate the correlation between CoT and TU models under this “zero-resistance” assumption. Our analysis revealed that modeling TU as a circuit with zero resistance of computational resistor increased the Power-accuracy Spearman correlation by over 10% compared to the original model, as illustrated in Figure 4b, which validates our hypothesis.

Furthermore, we hypothesize that PoT, leveraging programming languages, reduces planning resistance. As shown in Figure 4b, modeling PoT as a circuit with lower planning resistance achieved a correlation score exceeding 0.9423 between theoretical power and accuracy—significantly higher than TU. This finding highlights the superior effectiveness of PoT in improving model performance.

Self-consistency and Inference Scaling Law via Parallel Resistor in Circuits Self-consistency, as demonstrated by Wang et al. [40], utilizes multiple reasoning paths simultaneously, and determines final decision through majority voting, enhancing performance robustness and accuracy. Here, we interpret its effectiveness using a circuit model, which introduce parallelization of original resistors (R_{CoT}), significantly reducing the total system resistance. As shown in Figure 4c, the practical accuracy of the self-consistency strategy aligns closely with the theoretical output power curve, validating the correctness of our proposed model. Recent findings on the Inference Scaling Law [43, 28] further demonstrate that increasing the number of parallel samples, n , substantially improves accuracy. As n grows, the resistance value of CoT resistor approaches zero, optimizing the reasoning process. Further, when coverage introduces an absolutely correct answer verification process with zero resistance of verification resistor, exceeding the gains achieved by self-consistency alone. The alignment between theoretical predictions and empirical results, also evident in Figure 4c, reinforces the validity of this model. These results highlight the central role of self-consistency and inference scaling in enhancing the performance of circuits.

5 Exploration based on ECM

In this section, we primarily focus on how to use ECM to explore phenomena that have never been well explained and more novel prompting methods.

5.1 ICL Exploration

When Few-shot CoT Performs Worse than Zero-shot CoT? Despite the growing importance of ICL and CoT, a critical question remains: under what conditions is ICL essential, and when does zero-shot CoT suffice? To investigate this, we systematically examine the interaction between these two strategies. As shown in Figure 5a, our findings reveal a phenomenon we term “reverse ICL,” where demonstrations associated with a negative semantic magnetic field significantly impair the output power of circuits, thereby decreasing the model’s reasoning ability and resulting in worse performance compared to zero-shot CoT. This suggests that not all demonstrations contribute positively to the learning process. In contrast, demonstrations with a positive semantic magnetic field lead to an enhancement in performance. These results highlight the critical importance of

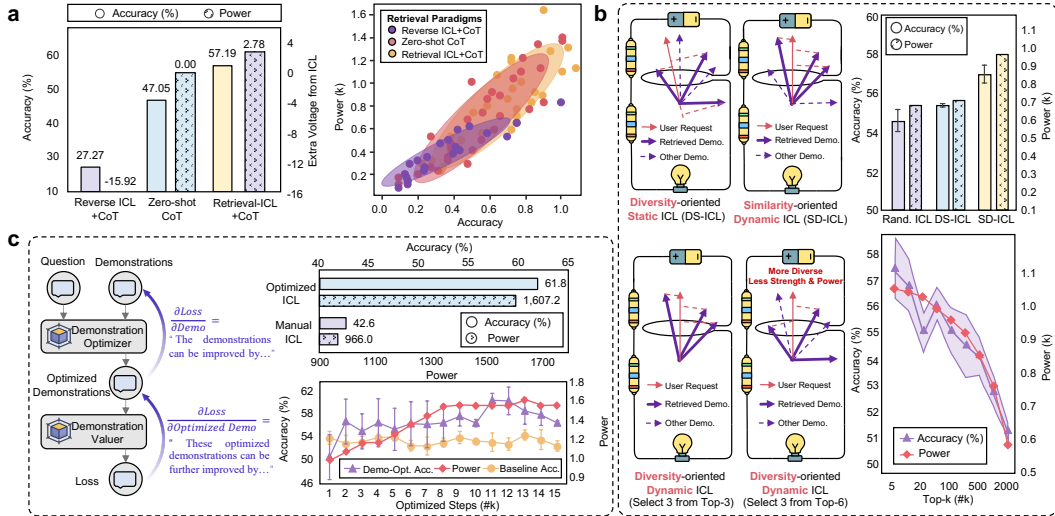


Figure 5: **The Experimental Exploration for ICL Strategies.**

a, The relationship between the introduction of demonstrations and model performance. Using Reverse ICL + CoT, which introduces demonstrations with negative magnetic fields, impairs the model’s reasoning ability and results in performance falling below that of Zero-shot CoT. In contrast, Retrieval-ICL + CoT, incorporating demonstrations with positive magnetic fields, significantly improves performance. **b**, The upper part of the figure contrasts Diversity-oriented Static ICL (DS-ICL), where demonstrations are retrieved for the whole task, and Similarity-oriented Dynamic ICL (SD-ICL), where demonstrations are retrieved for each request. In SD-ICL, demonstrations are more aligned with test requests, creating a stronger semantic magnetic field. The lower part highlights Diversity-oriented Dynamic ICL (DD-ICL), where increasing sampling range enhances the diversity but decreases the magnetic field strength of retrieved demonstrations, resulting in a more diverse but weaker strength, leading to less accuracy. **c**, The left figure illustrates the demo-optimization process, a methodology designed to refine the demonstrations used in ICL. The right figure shows that demo-optimization outperforms traditional prompt optimization by improving theoretical power.

selecting demonstrations based on their associated semantic magnetic field, which plays a crucial role in determining the success of ICL.

The influence of diversity in ICL retrieval: a static vs. dynamic perspective In ICL retrieval, two paradigms are commonly studied: static ICL, where the set of demonstrations remains fixed during testing, and dynamic ICL, where demonstrations are selected in real-time based on the specific test sample. Previous studies [19] reveal that semantic diversity in static ICL enhances performance by exposing the model to a broader range of contextual cues. Conversely, in dynamic ICL, diversity does not provide the same benefits and may even hinder performance [31]. This raises the question: *Why does diversity yield such contrasting outcomes in these retrieval modes?* To this end, we hypothesize that the benefits of diversity in static ICL can be likened to a magnetic field. Diverse demonstrations create a robust and expansive field, offering the model access to varied directional signals as test samples change. This broad-spectrum magnetic field stabilizes the model’s decision-making process, improving its generalizability and overall performance. As illustrated in Figure 5b, static ICL benefits from this diversity, which amplifies the model’s predictive power compared to random selection strategies. In dynamic ICL retrieval, however, the focus shifts toward selecting demonstrations closely aligned with the test sample. This approach optimizes the magnetic field for stronger, more targeted signals in the relevant direction. In this context, diversity becomes minimally critical; the alignment and intensity of retrieved demonstrations take precedence. As shown lower panel in Figure 5b, diverse but less aligned demonstrations enable less accuracy.

Demo-Optimization: a novel approach to enhance demonstration efficacy in ICL Recent advancements in prompt-based learning leverage feedback from outputs as model gradients, enabling large models to autonomously refine their prompts for more efficient learning [45]. Expanding on this foundation, we propose demo-optimization, a methodology tailored to optimize the demonstrations

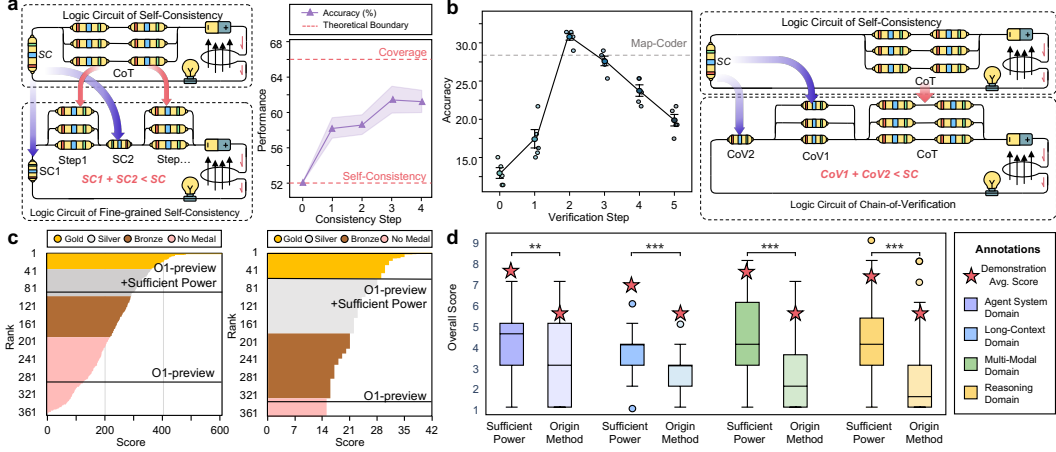


Figure 6: **Experimental Evaluation of Chain-of-Thought Strategies and Power-Optimized Performance on Complex Tasks**

a, Overview of the fine-grained self-consistency strategy in circuits. By decomposing parallel CoT resistors into smaller units, this approach effectively reduces overall circuit resistance value. **b**, Overview of the Chain-of-Verification (CoV) strategy in circuits. In addition to optimizing parallel CoT resistances, this method incorporates the concept of voting resistors in self-consistency to further reduce overall circuit resistance. The CoV strategy achieves this by sampling multiple voting results and validating them to finalize the decision. **c**, Leveraging stronger magnetic fields and reducing logical resistance significantly enhances circuit performance. The power-enhanced model achieved notable results in the IOI (left figure) and the IMO (right figure). **d**, The methodology for incorporating sufficient theoretical power into manual ratings during idea generation scenarios. This approach demonstrates a significant improvement over the original solution by enhancing the accuracy and reliability of the evaluation process.

used in ICL. Demo-optimization focuses on balancing the relative effectiveness between user requests and demonstrations (See Method for implementation details). As illustrated in Figure 5c, demo-optimization significantly outperforms traditional prompt optimization approaches, which primarily refine instructions. This method not only improves accuracy but also theoretically strengthens reasoning capabilities. Moreover, it addresses the persistent underfitting problem in prior ICL methods, offering a more precise and scalable strategy for enhancing demonstration-driven learning.

5.2 CoT Exploration

Optimize the same proportion of capabilities. The greater the original difficulty of the task corresponding to the capability, the greater the impact on the final performance. We can prove that optimizing a resistor with higher resistance to its original value $\frac{1}{k}$ results in a greater reduction in overall resistance of reasoning resistor R_{CoT} , yielding a more significant performance improvement compared to optimizing a lower resistance (See in Theoretical Proof). As shown in the meta-analysis in Appendix A, when solving questions that demand advanced planning, o1 [28]’s reasoning method, which emphasizes extensive exploration, significantly enhances the most challenging reasoning components. This improvement ultimately boosts overall performance on complex reasoning tasks. However, for tasks where the hardest component requires extensive domain-specific knowledge, insufficient optimization of such knowledge limits performance gains in those domains.

Fine-grained Self-consistency achieves better performance Easily, we can prove that, with a stable supply voltage, we can split a self-consistency ensemble into more fine-grained step-by-step self-consistency by conducting majority voting verification for each step, so that each resistance value of verification resistor can be smaller, and we can obtain larger output power (see Theoretical Proof). Indeed, as the number of self-consistency steps increases, the theoretical power value gradually increases. As shown in Figure 6a, the corresponding performance also gradually increases. At the same time, the corresponding upper bound and lower bound also satisfy the original self-consistency

and coverage. This not only proves the effectiveness of our proposed fine-grained self-consistency method but also proves the practical usability of the theoretical model.

Chain-of-Verification enhances model performance with parallelized verification resistors In conventional self-consistency frameworks, verification is typically conducted through series resistors. We propose an innovative approach, referred to as the “chain-of-verification,” which involves two key looped stages: first, verifying the correctness of individual outputs in parallel; and second, merging these verified results and subsequently meta-validating the correct to confirm the overall result of the merged outputs. It can enhance model performance by reducing the overall verification resistance. As depicted in Figure 6b, parallelization initially boosts performance by distributing verification tasks and lowering verification resistance. However, this improvement has limits. As parallelization increases, the overall resistors for parallel verifiers begins to rise. Beyond a critical threshold, this combined resistor surpasses the original self-consistency resistor, reversing the performance gains. As depicted in Figure 6b, this also demonstrates excessive chain-of-verification introduces diminishing returns. Thus, the chain-of-verification framework underscores the importance of balancing parallelization and resistor to optimize model verification efficiency.

6 Best Practice

To evaluate the impact of sufficient power on LLM performance, we analyzed its effects across three domains: the International Olympiad in Informatics (IOI), the International Mathematical Olympiad (IMO), and Natural Language Processing (NLP) idea generation using the AI-Scientist framework [23], by ensembling strategies outlined in Exploration Section. Our findings, shown in Figure 6c, demonstrate that augmenting the o1-preview model with enhanced power results in significant improvements. The power-enhanced o1-preview outperformed AlphaCode [20] and other state-of-the-art models on the IOI-level test set (code_contests [20]). Crucially, this boost consistently surpassed configurations lacking sufficient power, underscoring its pivotal role in model efficacy. In competitive contexts, such as IOI 2024 and IMO 2024, the powered o1-preview outperformed nearly 80% of global participants, earning silver and bronze medals. This highlights power as a decisive factor in high-stakes scenarios where traditional optimizations often fall short. Beyond correctness-focused tasks, as shown in Figure 6d, sufficient power also enhanced performance in creative challenges. For instance, in NLP-related idea-generation, it facilitates the better generation of novel and impactful research ideas (over 1 point of overall score improvement on average), expanding the potential of LLMs in both objective and subjective tasks.

7 Conclusion & Discussion

The Electronic Circuit Model (ECM) offers a unified framework for understanding and optimizing the ICL and CoT mechanisms, marking a significant advancement in LLM research. This framework elucidates model behavior while providing a quantifiable approach to enhance LLM performance. Our experiments demonstrate that ECM effectively captures model intricacies, serving as a reliable tool for analyzing and improving AI capabilities. Moreover, applying power-based optimization derived from ECM to advanced reasoning challenges, such as the International Olympiad in Informatics and the International Mathematical Olympiad, yielded superior results compared to leading competitors. These outcomes validate the theoretical foundation of ECM and highlight its transformative potential in improving AI reasoning and learning efficiency, with broad implications for next-generation intelligent systems.

8 Code Availability

The code and relevant data are available at <https://github.com/LightChen233/ECM>.

References

- [1] Josh Achiam, Steven Adler, Sandhini Agarwal, Lama Ahmad, Ilge Akkaya, Florencia Leoni Aleman, Diogo Almeida, Janko Altschmidt, Sam Altman, Shyamal Anadkat, et al. Gpt-4 technical report. *arXiv preprint arXiv:2303.08774*, 2023.

- [2] Tom Brown, Benjamin Mann, Nick Ryder, Melanie Subbiah, Jared D Kaplan, Prafulla Dhariwal, Arvind Neelakantan, Pranav Shyam, Girish Sastry, Amanda Askell, et al. Language models are few-shot learners. *Advances in neural information processing systems*, 33:1877–1901, 2020.
- [3] Yupeng Chang, Xu Wang, Jindong Wang, Yuan Wu, Linyi Yang, Kaijie Zhu, Hao Chen, Xiaoyuan Yi, Cunxiang Wang, Yidong Wang, et al. A survey on evaluation of large language models. *ACM Transactions on Intelligent Systems and Technology*, 2023.
- [4] Jianlv Chen, Shitao Xiao, Peitian Zhang, Kun Luo, Defu Lian, and Zheng Liu. Bge m3-embedding: Multi-lingual, multi-functionality, multi-granularity text embeddings through self-knowledge distillation. *arXiv preprint arXiv:2402.03216*, 2024.
- [5] Qiguang Chen, Libo Qin, Jiaqi WANG, Jingxuan Zhou, and Wanxiang Che. Unlocking the capabilities of thought: A reasoning boundary framework to quantify and optimize chain-of-thought. In *The Thirty-eighth Annual Conference on Neural Information Processing Systems*, 2024. URL <https://openreview.net/forum?id=pC44UMwy2v>.
- [6] Qiguang Chen, Libo Qin, Jin Zhang, Zhi Chen, Xiao Xu, and Wanxiang Che. M³CoT: A novel benchmark for multi-domain multi-step multi-modal chain-of-thought. In Lun-Wei Ku, Andre Martins, and Vivek Srikumar, editors, *Proceedings of the 62nd Annual Meeting of the Association for Computational Linguistics (Volume 1: Long Papers)*, pages 8199–8221, Bangkok, Thailand, August 2024. Association for Computational Linguistics. URL <https://aclanthology.org/2024.acl-long.446>.
- [7] Daixuan Cheng, Shaohan Huang, and Furu Wei. Adapting large language models via reading comprehension. In *The Twelfth International Conference on Learning Representations*, 2024. URL <https://openreview.net/forum?id=y886UXPEZ0>.
- [8] Karl Cobbe, Vineet Kosaraju, Mohammad Bavarian, Mark Chen, Heewoo Jun, Lukasz Kaiser, Matthias Plappert, Jerry Tworek, Jacob Hilton, Reiichiro Nakano, et al. Training verifiers to solve math word problems. *arXiv preprint arXiv:2110.14168*, 2021.
- [9] Jacob Devlin, Ming-Wei Chang, Kenton Lee, and Kristina Toutanova. BERT: Pre-training of deep bidirectional transformers for language understanding. In *Proceedings of the 2019 Conference of the North American Chapter of the Association for Computational Linguistics: Human Language Technologies, Volume 1 (Long and Short Papers)*, pages 4171–4186, Minneapolis, Minnesota, June 2019. Association for Computational Linguistics. doi: 10.18653/v1/N19-1423. URL <https://aclanthology.org/N19-1423>.
- [10] Aniket Rajiv Didolkar, Anirudh Goyal, Nan Rosemary Ke, Siyuan Guo, Michal Valko, Timothy P Lillicrap, Danilo Jimenez Rezende, Yoshua Bengio, Michael Curtis Mozer, and Sanjeev Arora. Metacognitive capabilities of LLMs: An exploration in mathematical problem solving. In *AI for Math Workshop @ ICML 2024*, 2024. URL <https://openreview.net/forum?id=0MsI3bSmmD>.
- [11] Qingxiu Dong, Lei Li, Damai Dai, Ce Zheng, Zhiyong Wu, Baobao Chang, Xu Sun, Jingjing Xu, and Zhifang Sui. A survey on in-context learning. *arXiv preprint arXiv:2301.00234*, 2022.
- [12] Abhimanyu Dubey, Abhinav Jauhri, Abhinav Pandey, Abhishek Kadian, Ahmad Al-Dahle, Aiesha Letman, Akhil Mathur, Alan Schelten, Amy Yang, Angela Fan, et al. The llama 3 herd of models. *arXiv preprint arXiv:2407.21783*, 2024.
- [13] Guhao Feng, Bohang Zhang, Yuntian Gu, Haotian Ye, Di He, and Liwei Wang. Towards revealing the mystery behind chain of thought: a theoretical perspective. *Advances in Neural Information Processing Systems*, 36, 2024.
- [14] Stefan Harrer. Attention is not all you need: the complicated case of ethically using large language models in healthcare and medicine. *EBioMedicine*, 90, 2023.
- [15] Mengkang Hu, Yao Mu, Xinmiao Chelsey Yu, Mingyu Ding, Shiguang Wu, Wenqi Shao, Qiguang Chen, Bin Wang, Yu Qiao, and Ping Luo. Tree-planner: Efficient close-loop task planning with large language models. In *The Twelfth International Conference on Learning Representations*, 2024.
- [16] Enkelejda Kasneci, Kathrin Seßler, Stefan Küchemann, Maria Bannert, Daryna Dementieva, Frank Fischer, Urs Gasser, Georg Groh, Stephan Günemann, Eyke Hüllermeier, et al. Chatgpt for good? on opportunities and challenges of large language models for education. *Learning and individual differences*, 103:102274, 2023.

- [17] Takeshi Kojima, Shixiang Shane Gu, Machel Reid, Yutaka Matsuo, and Yusuke Iwasawa. Large language models are zero-shot reasoners. In Alice H. Oh, Alekh Agarwal, Danielle Belgrave, and Kyunghyun Cho, editors, *Advances in Neural Information Processing Systems*, 2022. URL <https://openreview.net/forum?id=e2TBb5y0yFf>.
- [18] Tiffany H Kung, Morgan Cheatham, Arielle Medenilla, Czarina Sillos, Lorie De Leon, Camille Elepaño, Maria Madriaga, Rimel Aggabao, Giezel Diaz-Candido, James Maningo, et al. Performance of chatgpt on usmle: potential for ai-assisted medical education using large language models. *PLoS digital health*, 2(2):e0000198, 2023.
- [19] Xiaonan Li and Xipeng Qiu. Finding support examples for in-context learning. In Houda Bouamor, Juan Pino, and Kalika Bali, editors, *Findings of the Association for Computational Linguistics: EMNLP 2023*, pages 6219–6235, Singapore, December 2023. Association for Computational Linguistics. doi: 10.18653/v1/2023.findings-emnlp.411. URL <https://aclanthology.org/2023.findings-emnlp.411>.
- [20] Yujia Li, David Choi, Junyoung Chung, Nate Kushman, Julian Schrittwieser, Rémi Leblond, Tom Eccles, James Keeling, Felix Gimeno, Agustin Dal Lago, Thomas Hubert, Peter Choy, Cyprien de Masson d’Autume, Igor Babuschkin, Xinyun Chen, Po-Sen Huang, Johannes Welbl, Sven Gowal, Alexey Cherepanov, James Molloy, Daniel J. Mankowitz, Esme Sutherland Robson, Pushmeet Kohli, Nando de Freitas, Koray Kavukcuoglu, and Oriol Vinyals. Competition-level code generation with alphacode. *Science*, 378(6624):1092–1097, 2022. doi: 10.1126/science.abq1158. URL <https://www.science.org/doi/abs/10.1126/science.abq1158>.
- [21] Sheng Liu, Haotian Ye, Lei Xing, and James Y. Zou. In-context vectors: Making in context learning more effective and controllable through latent space steering. In *Forty-first International Conference on Machine Learning*, 2024. URL <https://openreview.net/forum?id=dJTChKgv3a>.
- [22] Yinhan Liu, Myle Ott, Naman Goyal, Jingfei Du, Mandar Joshi, Danqi Chen, Omer Levy, Mike Lewis, Luke Zettlemoyer, and Veselin Stoyanov. Roberta: A robustly optimized bert pretraining approach, 2019. URL <https://arxiv.org/abs/1907.11692>.
- [23] Chris Lu, Cong Lu, Robert Tjarko Lange, Jakob Foerster, Jeff Clune, and David Ha. The AI Scientist: Towards fully automated open-ended scientific discovery. *arXiv preprint arXiv:2408.06292*, 2024.
- [24] Aman Madaan, Katherine Hermann, and Amir Yazdanbakhsh. What makes chain-of-thought prompting effective? a counterfactual study. In *Findings of the Association for Computational Linguistics: EMNLP 2023*, pages 1448–1535, 2023.
- [25] Zabir Al Nazi and Wei Peng. Large language models in healthcare and medical domain: A review. In *Informatics*, volume 11, page 57. MDPI, 2024.
- [26] Maxwell Nye, Anders Johan Andreassen, Guy Gur-Ari, Henryk Michalewski, Jacob Austin, David Bieber, David Dohan, Aitor Lewkowycz, Maarten Bosma, David Luan, et al. Show your work: Scratchpads for intermediate computation with language models. In *Deep Learning for Code Workshop*, 2022.
- [27] OpenAI. Introducing chatgpt. 2022.
- [28] OpenAI. Learning to reason with llms. 2024. URL <https://openai.com/index/learning-to-reason-with-llms/>.
- [29] Wenbo Pan, Qiguang Chen, Xiao Xu, Wanxiang Che, and Libo Qin. A preliminary evaluation of chatgpt for zero-shot dialogue understanding, 2023.
- [30] Libo Qin, Qiguang Chen, Fuxuan Wei, Shijue Huang, and Wanxiang Che. Cross-lingual prompting: Improving zero-shot chain-of-thought reasoning across languages. *arXiv preprint arXiv:2310.14799*, 2023.
- [31] Libo Qin, Qiguang Chen, Hao Fei, Zhi Chen, Min Li, and Wanxiang Che. What factors affect multi-modal in-context learning? an in-depth exploration. In *The Thirty-eighth Annual Conference on Neural Information Processing Systems*, 2024. URL <https://openreview.net/forum?id=REVdYKGcfb>.
- [32] Libo Qin, Qiguang Chen, Xiachong Feng, Yang Wu, Yongheng Zhang, Yinghui Li, Min Li, Wanxiang Che, and Philip S. Yu. Large language models meet nlp: A survey, 2024.

- [33] Zhihong Shao, Yeyun Gong, Yelong Shen, Minlie Huang, Nan Duan, and Weizhu Chen. Synthetic prompting: Generating chain-of-thought demonstrations for large language models. In *International Conference on Machine Learning*, pages 30706–30775. PMLR, 2023.
- [34] Karthik Valmeekam, Matthew Marquez, Alberto Olmo, Sarath Sreedharan, and Subbarao Kambhampati. Planbench: An extensible benchmark for evaluating large language models on planning and reasoning about change. In *Thirty-seventh Conference on Neural Information Processing Systems Datasets and Benchmarks Track*, 2023. URL <https://openreview.net/forum?id=YXogl4uQU0>.
- [35] Karthik Valmeekam, Kaya Stechly, and Subbarao Kambhampati. LLMs still can’t plan; can LRMs? a preliminary evaluation of openAI’s o1 on planbench. In *NeurIPS 2024 Workshop on Open-World Agents*, 2024. URL <https://openreview.net/forum?id=Gcr1Lx4Koz>.
- [36] Johannes Von Oswald, Eyvind Niklasson, Ettore Randazzo, João Sacramento, Alexander Mordvintsev, Andrey Zhmoginov, and Max Vladymyrov. Transformers learn in-context by gradient descent. In *International Conference on Machine Learning*, pages 35151–35174. PMLR, 2023.
- [37] Boshi Wang, Sewon Min, Xiang Deng, Jiaming Shen, You Wu, Luke Zettlemoyer, and Huan Sun. Towards understanding chain-of-thought prompting: An empirical study of what matters. In *Proceedings of the 61st Annual Meeting of the Association for Computational Linguistics (Volume 1: Long Papers)*, pages 2717–2739, 2023.
- [38] Lean Wang, Lei Li, Damai Dai, Deli Chen, Hao Zhou, Fandong Meng, Jie Zhou, and Xu Sun. Label words are anchors: An information flow perspective for understanding in-context learning. In Houda Bouamor, Juan Pino, and Kalika Bali, editors, *Proceedings of the 2023 Conference on Empirical Methods in Natural Language Processing*, pages 9840–9855, Singapore, December 2023. Association for Computational Linguistics. doi: 10.18653/v1/2023.emnlp-main.609. URL <https://aclanthology.org/2023.emnlp-main.609>.
- [39] Xinyi Wang, Wanrong Zhu, and William Yang Wang. Large language models are implicitly topic models: Explaining and finding good demonstrations for in-context learning. *arXiv preprint arXiv:2301.11916*, page 3, 2023.
- [40] Xuezhi Wang, Jason Wei, Dale Schuurmans, Quoc V Le, Ed H. Chi, Sharan Narang, Aakanksha Chowdhery, and Denny Zhou. Self-consistency improves chain of thought reasoning in language models. In *The Eleventh International Conference on Learning Representations*, 2023. URL <https://openreview.net/forum?id=1PL1NIMMrw>.
- [41] Jason Wei, Xuezhi Wang, Dale Schuurmans, Maarten Bosma, brian ichter, Fei Xia, Ed H. Chi, Quoc V Le, and Denny Zhou. Chain of thought prompting elicits reasoning in large language models. In Alice H. Oh, Alekh Agarwal, Danielle Belgrave, and Kyunghyun Cho, editors, *Advances in Neural Information Processing Systems*, 2022. URL https://openreview.net/forum?id=_VjQLMeSB_J.
- [42] Siwei Wu, Zhongyuan Peng, Xinrun Du, Tuney Zheng, Minghao Liu, Jialong Wu, Jiachen Ma, Yizhi Li, Jian Yang, Wangchunshu Zhou, et al. A comparative study on reasoning patterns of openai’s o1 model. *arXiv preprint arXiv:2410.13639*, 2024.
- [43] Yangzhen Wu, Zhiqing Sun, Shanda Li, Sean Welleck, and Yiming Yang. Inference scaling laws: An empirical analysis of compute-optimal inference for problem-solving with language models. *arXiv preprint arXiv:2408.00724*, 2024.
- [44] Zhilin Yang, Peng Qi, Saizheng Zhang, Yoshua Bengio, William Cohen, Ruslan Salakhutdinov, and Christopher D. Manning. HotpotQA: A dataset for diverse, explainable multi-hop question answering. In Ellen Riloff, David Chiang, Julia Hockenmaier, and Jun’ichi Tsujii, editors, *Proceedings of the 2018 Conference on Empirical Methods in Natural Language Processing*, pages 2369–2380, Brussels, Belgium, October–November 2018. Association for Computational Linguistics. doi: 10.18653/v1/D18-1259. URL <https://aclanthology.org/D18-1259>.
- [45] Mert Yuksekgonul, Federico Bianchi, Joseph Boen, Sheng Liu, Zhi Huang, Carlos Guestrin, and James Zou. Textgrad: Automatic" differentiation" via text. *arXiv preprint arXiv:2406.07496*, 2024.
- [46] Wayne Xin Zhao, Kun Zhou, Junyi Li, Tianyi Tang, Xiaolei Wang, Yupeng Hou, Yingqian Min, Beichen Zhang, Junjie Zhang, Zican Dong, et al. A survey of large language models. *arXiv preprint arXiv:2303.18223*, 2023.

- [47] Ziyu Zhuang, Qiguang Chen, Longxuan Ma, Mingda Li, Yi Han, Yushan Qian, Haopeng Bai, Zixian Feng, Weinan Zhang, and Ting Liu. Through the lens of core competency: Survey on evaluation of large language models. *arXiv preprint arXiv:2308.07902*, 2023.

A Method Implementation Details

A.1 Theoretical Model

Faraday’s Law of In-Context Learning In-context learning (ICL) can be likened to the behavior of a semantic magnetic field generated by a sub-power source, as described by Faraday’s Law. The positive direction of the semantic magnetic field is defined by the query semantic vector \vec{S}_q . Given N context samples represented by semantic vectors \vec{S}_i , the total semantic magnetic field strength Φ_0^B experienced by the model is the projection of these vectors onto \vec{S}_q . Mathematically:

$$\Phi_0^B = \sum_{i=1}^N \cos \theta_{qi} \cdot |\vec{S}_i| = \sum_{i=1}^N \frac{\vec{S}_q \cdot \vec{S}_i}{|\vec{S}_q|} \quad (4)$$

where $\cos \theta_{qi}$ represents the angle between \vec{S}_q and \vec{S}_i .

As new context samples are processed, the semantic field strength Φ_0^B is hypothesized to decay linearly over time:

$$\Phi^B(t) = -\lambda \Phi_0^B t, \quad (5)$$

where λ is the decay constant representing the rate at which the model forgets or absorbs information. According to Faraday’s Law of electromagnetic induction, the rate of change in the semantic magnetic field induces an electromotive force, which drives effective ICL. With a time step Δt for each reasoning step, the induced EMF, \mathcal{E}_{ICL} , is:

$$\mathcal{E}_{\text{ICL}} = -\frac{\Delta \Phi^B(t)}{\Delta t} = \lambda \Phi_0^B. \quad (6)$$

Substituting Φ_0^B into this equation yields:

$$\mathcal{E}_{\text{ICL}} = \lambda \sum_{i=1}^N \frac{\vec{S}_q \cdot \vec{S}_i}{|\vec{S}_q|}. \quad (7)$$

In conclusion, this analogy offers a structured framework to analyze how information flows during ICL. By extending the dynamics of ICL through the principles of electromagnetic induction, we provide a mathematical model to explain how models incorporate and gradually forget information as they process contextual examples.

Ohm’s Law of Chain-of-Thought In this framework, each sub-difficulty of a model introduces a distinct level of difficulty, analogous to resistors in series. Formally, following Chen et al. [5], the ease with which a model can solve a particular task is represented by its reasoning boundary. Let \mathcal{B}_{CoT} denote the overall reasoning boundary of a Chain-of-Thought process, and \mathcal{B}_i denote the reasoning boundary of the i -th sub-capability. The overall reasoning boundary can be expressed by the harmonic sum:

$$\mathcal{B}_{\text{CoT}} = \frac{1}{\sum_{i=1}^K \frac{1}{\mathcal{B}_i}}, \quad (8)$$

where K denotes the number of sub-capabilities. Reasoning resistor, R , quantifies the difficulty of a reasoning process and is mathematically defined as the reciprocal of the reasoning boundary. A higher boundary corresponds to an easier problem and lower resistor. Specifically, we define the sub-difficulty of the i -th sub-task as:

$$R_i = \frac{1}{\mathcal{B}_i}. \quad (9)$$

Substituting this into Equation 8, the total reasoning resistor for the CoT process is expressed as:

$$R_{\text{CoT}} = \sum_{i=1}^K R_i, \tag{10}$$

where R_{CoT} represents the combined difficulty, analogous to total resistor in a series circuit. Overall, the CoT reasoning framework is further formalized by the Ohm’s law analogy:

$$I_{\text{model}} = \frac{\mathcal{E}_{\text{model}} + \mathcal{E}_{\text{ICL}}}{R_{\text{CoT}} + R_0}, \tag{11}$$

where R_0 denotes a output resistor with static resistance value. This modular formulation effectively quantifies cognitive task complexity through combined reasoning resistor.

A.2 Genral Experimental Settings

All experiments, unless stated otherwise, are conducted on GPT-3.5-Turbo. Following Wei et al. [41], CoT experiments select 5 manually constructed demonstrations for all multi-step reasoning tasks. *Top-p* is selected from {0.95, 1}, and *Temperature* is selected in range [0, 1] for robustness evaluation. Experiments are primarily conducted on the BIGGSM dataset [5], a benchmark for mathematical reasoning. In ICL, demonstrations are dynamically retrieved using a 5-shot approach from the GSM8K development dataset [8] by default. To formalize the demonstration selection process, we retrieve the semantic magnetic field strength Φ_0^B by default, as defined in Eq. 4. All demonstration representation methods employ the meta-recognition [10] framework by default: GPT-4o [1] extracts sub-capability tags, and Roberta [22] concatenates and represents these tags in the hidden space. In addition, only the magnetic field strength Φ_0^B is calculated and the resistor value R_{CoT} directly adopts the fitting values from Chen et al. [5]. In addition, other parameters are fitted values using the verification set. Different models fit different voltages $\mathcal{E}_{\text{model}}$. The whole experiment shares a R_0 value. Different demonstration representation methods have different λ . All experiments involving variance were sampled 3 times at different temperatures.

A.3 Model Verification Experiment Details

CoT Ohm’s Law Verification To validate the Ohm’s Law assumption in the CoT approach, we conduct the following experiment. To eliminate potential interference from ICL and ensure effective stimulation of CoT capabilities, we append the phrase “Let’s think step-by-step!” to the user query. This adjustment aims to stimulate and isolate the CoT mechanism and prevent ICL-related influences. We then perform sampling based on power levels from the BIGGSM dataset, using 30-unit intervals to map calculated power to accuracy². To reduce random errors and ensure sufficient sampling points, we retain data points with at least 10 samples. Accuracy is calculated for each sampling interval to analyze the relationship between power levels and model performance, enabling an effective evaluation of the correlation between sampling power and accuracy.

ICL Faraday’s Law Verification To validate the semantic magnetic field hypothesis in ICL, we observe that without CoT reasoning, performance on complex mathematical tasks often declines to near-zero levels, thereby cannot easily observe their relevance. Thus, this experiment incorporates both CoT reasoning and ICL. While the CoT reasoning format remains constant, we focus on varying the similarity measures used for sample retrieval through ICL. The central adjustment involves applying different similarity measures for sample retrieval, directly affecting the model’s performance on complex tasks. These measures also help calculate the additional “voltage” introduced by semantic magnetic fields, quantifying their influence on performance. All demonstration representation methods employ BGE [4] to represent the request in the hidden space.

Unified circuit mechanism verification To further validate the effectiveness of our unified framework for modeling ICL and CoT, we conduct experiments integrating both paradigms into different retrieval settings. These experiments test the robustness and rationality of the proposed theoretical framework. Specifically, we examine three retrieval methods: random retrieval, forward magnetic

²The absolute power values are meaningless due to inconsistencies in semantic space scaling across encoding methods. However, their relative values within a method correlate positively with real accuracy.

field retrieval, and reverse magnetic field retrieval. In the random retrieval setup, samples are selected randomly from the development set as ICL demonstrations for each test sample. The Retrieval-ICL selects samples with maximized magnetic field intensity in the corresponding test sample’s direction. Conversely, the Reverse-ICL focuses on samples with minimal (even negative) magnetic field intensity, enabling exploration of contrasting ICL examples. This comprehensive validation highlights the robustness of our framework across diverse retrieval strategies and empirically demonstrates its generalizability in both ICL and CoT scenarios.

Extension Experiment Details on Various Models and Tasks To further enhance the applicability of ECM, we conducted experiments across a series of models, where each model was designed to fit specific baseline voltage values, Φ_0^B , and compute the corresponding power output. Subsequently, all models were consolidated onto a single graph, enabling us to analyze the correlation between output power and relative accuracy. As illustrated in Figure x, the results reveal clear and detailed correlations across the models. However, when accuracy exceeds 90%, the scarcity of samples requiring sufficient power in this range, likely due to limitations in the dataset, leads to poor fitting in this region.

Furthermore, our experiments on HotpotQA and Medical Probing closely adhered to the experimental settings established by Chen et al. [5]. However, since Medical Probing includes rationale annotations limited to background knowledge rather than chain reasoning, we supplemented portions of the reasoning process to facilitate a more precise correlation analysis. Additionally, the data for robotic planning was directly extracted from the running logs provided by Valmeekam et al. [34].

A.4 Model Explanation Experiments

A.4.1 ICL Explanation

Embedder Comparison To evaluate how different embedders influence model performance, we replace the sample encoder with BERT [9], RoBERTa [22], and BGE [4]. These embeddings are used for sample retrieval in ICL to minimize potential biases that may arise if a single embedder disproportionately emphasizes specific data features. For instance, an embedder might favor samples aligned with its encoding patterns, leading to distortions in the relationship between retrieved representations and model performance. By employing diverse embedders, we aim to mitigate such biases and promote more accurate theoretical modeling for ICL.

Synthetic-CoT Implementation This section examines the implementation of *Synthetic-CoT* within the ECM framework to assess its impact on reasoning performance. *Synthetic-CoT* autonomously generates in-context demonstrations with chain-of-thought reasoning paths. We hypothesize that these demonstrations align the system’s magnetic field, reducing logical resistor and enhancing overall circuit power output. To validate this, we generate a series of demonstrations with two categories by *Synthetic-CoT*, including:

- **Positive Magnetic Field Demonstrations:** In-context demonstrations generated by *Synthetic-CoT* are positively aligned with the magnetic polarity of user queries direction.
- **Negative Magnetic Field Demonstrations:** In-context demonstrations generated by *Synthetic-CoT* are with opposing magnetic polarity of user queries direction.

We analyze the magnetic field contributions of these categories, focusing on their differing effects. Subsequently, we integrate the computed power and measured accuracy to further investigate their operational mechanisms.

A.4.2 CoT Explanation

Direct answer output We analyze the effect of *direct answer output* on reasoning performance through the ECM framework. This approach bypasses intermediary reasoning steps by appending the directive, “Let’s directly output the result without additional reasoning content,” which generates significant logical resistor within the system. To quantify this, we gradually improve the resistance value of reasoning resistor R_{CoT} , which meets largest Spearman correlations in the validation set, and employ the R_{CoT} to the test set.

Tool-Usage and PoT We further investigate how *Tool-Usage* and *Program-of-Thought (PoT)* mitigate specific resistors in the reasoning process, focusing on their impact under the ECM framework on computational and planning resistors:

- **Tool-Usage:** Tool-Usage aims to reduce *computational resistor* by offloading complex calculations to external tools. Modeled as a zero-resistor computational circuit in our experiments, Tool-Usage enhances the Power-Accuracy Spearman correlation.
- **Program-of-Thought (PoT):** PoT targets *planning resistor* by employing structured programming logic to enable clearer and more efficient reasoning. This advantage stems from PoT’s superior ability to reduce planning resistor, facilitating finer-grained logical alignment.³

These findings confirm that while Tool-Usage primarily addresses single-step computational resistor, PoT excels in optimizing overall planning resistor. Both methods significantly enhance performance within the ECM framework, highlighting their complementary contributions to reducing resistor and improving reasoning capabilities.

Self-consistency and Coverage Design This experiment evaluated the self-consistency strategy proposed by Wang et al. [40], which employs multiple parallel reasoning paths and a majority-vote mechanism for the final decision. This strategy is hypothesized to enhance performance by reducing the system’s resistance to diverse inputs, analogous to parallel resistors in a circuit, where total resistor decreases compared to series connections. By applying this analogy, we demonstrate how parallel reasoning can lower cognitive load, improving accuracy and efficiency in decision-making.

To examine the influence of inference scaling on model performance, we investigated the relationship between the number of parallel samples, k , and the metric like Accuracy or Pass@ k , as described in the Inference Scaling Law. Specifically, Pass@ k measures the accuracy of Coverage method which obtains a correct result when at least one sampled prediction is accurate. We modeled the reasoning process as a resistive circuit, where each sample represents a parallel resistor. As k increases, the resistance of reasoning resistor approaches zero, reflecting a refined reasoning process and enhanced accuracy. Further, Coverage methods introduce zero verification resistance introduce much less overall resistance values, larger output power, and higher related performance. The experiment systematically varied k from 1 to 100 in increments of 5, recording the accuracy and Pass@ k metric under each condition⁴. We track individual reasoning path resistance, comparing these values with observed accuracy to validate the circuit analogy. The effectiveness of Self-consistency and Coverage methods can be mathematically proved based on the ECM detailed in Theoretical Proof.

A.5 Model Exploration Experiments

A.5.1 ICL Exploration

Diversity This study examines the differing impacts of semantic diversity on static and dynamic ICL retrieval. We map all samples into the hidden space using RoBERTa. In static ICL, we employ a fixed set of demonstrations with the highest semantic diversity across the task, hypothesizing that this diversity enhances model performance by providing a wider range of contextual cues. In contrast, dynamic ICL selects demonstrations in real-time based on the test sample’s characteristics, prioritizing semantically similar examples that align closely with the input. To test these, we evaluate both retrieval strategies. For static ICL, we compare models exposed to high-diversity and random demonstration sets, measuring performance using accuracy. For dynamic ICL, we contrast random selection with retrieval strategies emphasizing semantic alignment. We hypothesize that semantic diversity improves static ICL by stabilizing decision-making, while in dynamic ICL, retrieving highly relevant demonstrations yields better accuracy. In addition, in order to prove that diversity is ineffective in the setting of dynamic ICL, we sort the semantic magnetic field strength and select as diverse samples as possible among the top- k samples as ICL demonstrations.

Demo-Optimization This experiment introduces demo-optimization, a novel method for optimizing demonstrations in ICL. The approach dynamically refines demonstrations based on feedback from the LLM’s outputs, which serve as gradients for improvement. Specifically, initial ICL demonstrations

³All implementation prompts come from Chen et al. [5]

⁴We remove those generated samples are totally the same to keep the independent sampling.

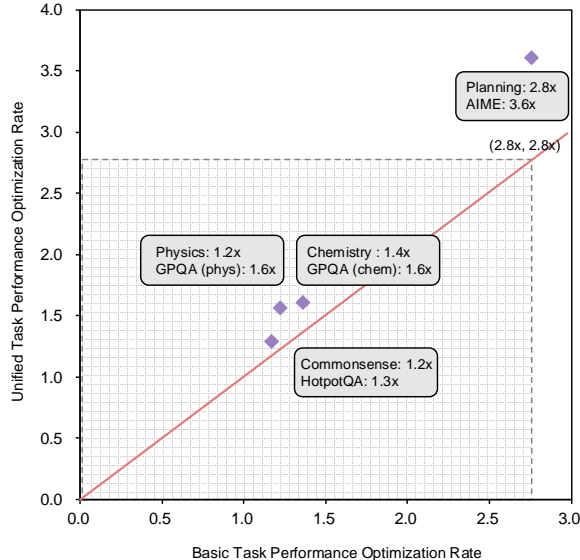


Figure 7: Meta-analysis for the model improvements on different tasks. The data comes from Wu et al. [42], Valmeekam et al. [35] and OpenAI [28]. We collect evaluation data related to plan and knowledge based on OpenAI [28]. In addition, we remove data points with final results exceeding 90%, because these data have exceeded human levels, resulting in potential labeling bias and test set labeling errors.

in prompting are selected, with both development dataset for optimization and optimization prompt configurations prepared. A feedback loop guides adjustments to the demonstrations, improving their clarity, relevance, and alignment with prompt requirements. Demonstrations are iteratively refined, and evaluated for contextual alignment with user requests in the development dataset. The method is compared against static and whole-prompt-optimized baselines, with performance assessed using task accuracy, output consistency, and learning efficiency.

A.5.2 CoT Exploration

CoT Optimization Proportion To evaluate the improvement in reasoning resistance R_i to the target level of $\frac{1}{k}$, which depends heavily on the task’s reasoning demands, we conducted a meta-analysis of experimental results from diverse datasets. These datasets are divided into two main categories: (1) tasks requiring advanced planning and logical reasoning, such as mathematical derivations and multi-hop question answering, and (2) tasks reliant on extensive domain-specific knowledge, such as chemistry and physical question answering. As shown in Figure 7, our meta-analysis demonstrates that tasks requiring advanced planning gain the most from enhanced exploratory reasoning, significantly improving challenging components (e.g., a 2.8-fold optimization in planning capability) and overall task performance (e.g., a 3.6-fold optimization on AIME, a benchmark emphasizing long-term planning). In contrast, tasks relying heavily on domain-specific knowledge exhibit limited improvement without targeted optimization in those areas. This underscores the importance of domain-aware reasoning strategies. For example, tasks involving complex reasoning and knowledge integration, such as GPQA (chemistry, physics) and HotpotQA, show performance improvements directly proportional to advancements in the related knowledge domains (approximately 1:1 ratio). The effectiveness and the underlying reasons for such phenomena can be mathematically analyzed and proved based on the ECM detailed in Theoretical Proof.

Fine-grained Self-consistency In this experiment, we examine how decomposing a self-consistency ensemble into smaller, incremental majority-voting steps reduces reasoning resistor in circuits, compared to the conventional single-step approach. The circuit operates at a stable supply voltage of 5 units, and reasoning resistance value and output power are evaluated as the number of steps increases. Each majority-voting step simplifies logical complexity and reduces overall resistance by incorporating less verification resistance in the decision-making process. Our findings demon-

strate a consistent decline in reasoning resistance alongside a rise in output power, confirming that finer-grained majority-voting processes improve both efficiency and power output in circuits. The effectiveness of this method can be mathematically proved based on the ECM detailed in Theoretical Proof.

Chain-of-Verification Traditional self-consistency frameworks rely on a sequential verification model, where each step depends on the completion of the previous one. This structure often incurs high computational costs, as subsequent tasks cannot begin until earlier ones are resolved. To overcome this limitation, we introduce the “chain-of-verification (CoV),” a novel strategy that parallelizes verification tasks into independent components. Each component operates concurrently, validating distinct parts of the system without interdependence. This parallel approach reduces overall computational resistance by distributing the workload across multiple verifiers, thereby enabling more effective validation. As illustrated in Figure 6b, parallelization not only accelerates the verification process but also enhances model performance by mitigating bottlenecks. This improvement is particularly pronounced in large-scale systems, where sequential verification would otherwise impede efficiency. The effectiveness of CoV can also be mathematically proved based on the ECM detailed in Theoretical Proof.

A.6 Best Practice

In practice, we integrate all proposed strategies into the O1-preview model to address IOI, IMO problem-solving, and idea-generation tasks for much less resistance value of planning resistor.

IOI Task For the IOI task, we employ the following methods: First, using O1-preview, we maximize the optimization of the resistance value of its “planning resistor.” Additionally, five high-intensity semantic field problems from the code_contest training dataset are retrieved as demonstrations, boosting the voltage supplied by additional ICL fields. Second, we apply the Coverage technique, sampling 100 instances and leveraging both provided and model-generated test cases in parallel, effectively reducing resistance in chain-of-thought reasoning. This process, executed in parallel, effectively reduces the resistance in the chain-of-thought reasoning. Furthermore, we incorporate the CoV concept to iteratively validate the final outputs, thereby optimizing the final performance. Additionally, the CoV framework is employed to iteratively validate outputs and optimize overall performance. To prevent data leakage from competition datasets in C++, competition code is generated in Python. Manual adjustments ensure compatibility between Python and C++ input/output handling, preserving the core logic for fair comparative testing.

IMO Task A similar approach is adopted for the IMO task. O1-preview is optimized for planning resistor, and five high-intensity semantic field problems from past IMO datasets are retrieved as demonstrations to enhance ICL field voltage. The Coverage technique is again employed, sampling 100 instances in parallel to reduce reasoning resistance. We introduce the fine-grained self-consistency approach within the CoV framework, enabling iterative validation of outputs and achieving notable performance gains. Additionally, we only evaluate answers and do not consider process scores.

Idea-Generation Task We utilize the AI Scientist framework [23] to generate over 10 ideas per domain and draft academic papers, limited to the abstract and introduction sections to address ethical concerns by avoiding experimental claims. A 16-member review panel, including 2 Superior reviewers (6+ years of experience), 8 Senior reviewers (4+ years), and 6 Junior reviewers (2+ years), ensures reliability. Each paper is reviewed by at least four reviewers, including two Senior or Superior reviewers, following NeurIPS guidelines. High-quality examples with strong semantic fields, sourced from past ICLR, NeurIPS, and CoLM openreview data, are used to guide generation. The Coverage technique, sampling of 100 instances, and iterative validation through the CoV framework further refine the process.

A.7 Internal Mechanism underlying the ECM

To investigate the internal mechanisms underlying ECM, we conduct experiments in the LLaMA3-8B [12] focusing on three strategies: Zero-shot CoT, ICL with Semantic Magnetic Field Retrieval, and PoT. By analyzing neuron activation values and frequencies—particularly in the most activated

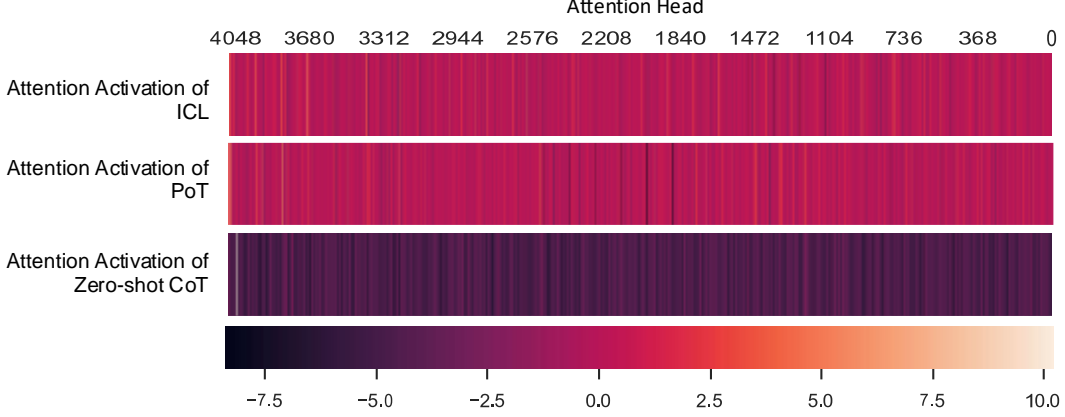


Figure 8: Neuron activation heatmaps for the most activated attention layer under three reasoning strategies: (a) Zero-shot CoT, (b) ICL with Semantic Magnetic Field Retrieval, and (c) Program of Thought (PoT).

attention layer—we aim to elucidate the relationship between reasoning strategies and neural dynamics. These findings support the theoretical framework of ECM. The experiments use the BigGSM dataset, a standard benchmark for mathematical reasoning tasks. For ICL, demonstrations are dynamically retrieved using the BGE model in a 3-shot configuration. Figure 8 shows neuron activation heatmaps for the most activated attention layer under each reasoning strategy. For Zero-shot CoT, the heatmap reveals sparse activations, with limited regions of intense activity, highlighting the difficulty of reasoning without contextual support. Conversely, ICL and PoT display more distributed and elevated activation patterns. These suggest that the underlying reasoning mechanisms engage a broader spectrum of neurons, with comparable activation dynamics reflecting similar reasoning power across these strategies.

B Theoretical Proof

B.1 Analysis of Effectiveness of Self-consistency and Coverage Design

B.1.1 Analysis of Effectiveness of Self-consistency

First, according to the series resistor assumption of CoT, the total resistance of series resistors can be expressed as:

$$R_{\text{all}} = R_0 + R_{\text{CoT}}. \quad (12)$$

Building upon the illustration in Figure 4c, we hypothesize that self-consistency, achieved through multiple parallel reasoning processes and subsequent result aggregation by majority voting, can be represented as an aggregation resistor integrated alongside several parallel CoT resistors. In this framework, the effective resistance of the reasoning process transitions from R_{CoT} to $\frac{1}{\sum_{i=1}^n \frac{1}{R_{\text{CoT}}^i}}$, accompanied with a majority-voting resistor R_S to determine the final outcome. Consequently, the total resistance associated with self-consistency, denoted as R'_{all} , is expressed as:

$$R'_{\text{all}} = R_0 + R_S + \frac{1}{\sum_{i=1}^n \frac{1}{R_{\text{CoT}}^i}}, \quad (13)$$

where n is the number of samples, R_{CoT}^i denotes the resistance corresponding to the i -th sample and R_S accounts for the resistor due to self-consistency integration. This framework allows for rapid computation of the output power:

$$P_{\text{out}}^{\text{self}} = \frac{(\mathcal{E}_{\text{model}} + \mathcal{E}_{\text{ICL}})^2 R_0}{(R_0 + R_S + \frac{1}{\sum_{i=1}^n \frac{1}{R_{\text{CoT}}^i}})^2}. \quad (14)$$

As the number of samples increases, the curves in Figure 4c reveal that the real performance curve is almost exactly consistent with the theoretical range. Furthermore, assume that $\{R_{\text{CoT}}^i\}_{i=1}^{\infty}$ is bounded

thus we can easily prove that the overall resistance has a lower bound:

$$\lim_{n \rightarrow +\infty} R'_{\text{all}} = R_0 + R_S + \lim_{n \rightarrow +\infty} \frac{1}{\sum_{i=1}^n \frac{1}{R_{\text{CoT}}^i}} = R_0 + R_S. \quad (15)$$

The corresponding performance bound is:

$$\hat{P}_{\text{out}}^{\text{self}} = \frac{(\mathcal{E}_{\text{model}} + \mathcal{E}_{\text{ICL}})^2 R_0}{(R_0 + R_S)^2} \quad (16)$$

As shown in Figure 4c, model performance aligns with this theoretical upper bound as sample size increases.

B.1.2 Analysis of Effectiveness of Coverage Design

Similarly, we hypothesize that coverage can be considered correct if at least one of multiple parallel reasoning is accurate. Under this assumption, the integration difficulty in self-consistency verification approaches zero. Analogously, this can be modeled as a zero-value combined resistance in parallel with multiple CoT resistors, where the coverage resistance of self-consistency \hat{R}_{all} is given by:

$$\hat{R}_{\text{all}} = R_0 + R_S + \frac{1}{\sum_{i=1}^n \frac{1}{R_{\text{CoT}}^i}} = R_0 + \frac{1}{\sum_{i=1}^n \frac{1}{R_{\text{CoT}}^i}} \quad (17)$$

where n denotes the number of samples. Using this, the theoretical output power can be similarly calculated as:

$$P_{\text{out}}^{\text{cover}} = \frac{(\mathcal{E}_{\text{model}} + \mathcal{E}_{\text{ICL}})^2 R_0}{\left(\frac{1}{\sum_{i=1}^n \frac{1}{R_{\text{CoT}}^i}} + R_0\right)^2}, \quad (18)$$

which are much more smaller than $P_{\text{out}}^{\text{self}}$ in the same n sample size with $R_S \gg 0$. As the number of samples increases, the curve in Figure 4c demonstrates that the real performance aligns closely with the theoretical range. Building upon the same bounded assumption of $\{R_{\text{CoT}}^i\}_{i=1}^{\infty}$, this setup also defines a resistance lower bound:

$$\lim_{n \rightarrow +\infty} \hat{R}_{\text{all}} = R_0 + \lim_{n \rightarrow +\infty} \frac{1}{\sum_{i=1}^n \frac{1}{R_{\text{CoT}}^i}} = R_0 \quad (19)$$

and the corresponding lower-bound performance:

$$\hat{P}_{\text{out}}^{\text{cover}} = \frac{(\mathcal{E}_{\text{model}} + \mathcal{E}_{\text{ICL}})^2}{R_0}. \quad (20)$$

As shown in Figure 4c, the model's performance gradually converges toward this upper bound and much larger than the performance of self-consistency, demonstrating consistency with the theoretical predictions.

NOTE According to the theoretical formulation in Eq. 18, in the reasoning phase where the resistance is significantly greater than R_0 , the overall trend shows that Coverage is approximately proportional to the number of samples. Meanwhile, certain Inference Scaling Laws indicate that Coverage and the logarithm of the number of samples exhibit an approximately proportional relationship. These two observations are not contradictory, as our model assumes relatively independent sampling. However, we have observed that when the number of samples exceeds 100, an increasing proportion of the samples become duplicates rather than independent samples. Consequently, the probability of generating new samples follows the trend where n samples are expected to yield approximately $\log n$ distinct reasoning samples.

B.2 Analysis of Effectiveness of Fine-grained Self-consistency

According to Eq. 13, the original circuit can be considered as a large parallel reasoning and verification process and the total resistor is as follows:

$$R'_{\text{all}} = R_0 + R_S + \frac{1}{\sum_{i=1}^n \frac{1}{R_{\text{CoT}}^i}}. \quad (21)$$

As shown in Figure 6a, this process is decomposed into multiple sequential, smaller-scale parallel reasoning and verifications. This refinement transforms *a single large parallel reasoning resistance with significant verification resistance* into *a sequence of smaller parallel reasoning resistance and smaller verification resistance*. Formally, this is expressed as:

$$R_{\text{all}}^{\text{fine}} = R_0 + \sum_j R_j^S + \sum_j \frac{1}{\sum_{i=1}^n \frac{1}{R_j^i}}, \quad (22)$$

where n denotes the sampling size, R_j^S represents the small and fine-grained verification resistance for j -th step, and R_j^i corresponds to smaller reasoning resistance for j -th step for i -th sampling. The total resistance can be broken down into resistance of sub-step resistor as $R_{\text{CoT}}^i = \sum_j R_j^i$.

We aim to demonstrate that our approach indeed optimizes the total resistance, i.e., $R_{\text{all}}^{\text{fine}} < R'_{\text{all}}$. To prove this, we need to show that $R_{\text{all}}^{\text{fine}} - R'_{\text{all}} < 0$. The proof is as follows:

$$R_{\text{all}}^{\text{fine}} - R'_{\text{all}} = \sum_j R_j^S - R_S + \frac{R_{\text{CoT}}}{n} - \sum_j \frac{R_j^i}{n} \quad (23)$$

$$= \sum_j R_j^S - R_S. \quad (24)$$

It is evident that verifying correctness at the individual step level is simpler than verifying the correctness of the entire chain, so $\sum_i R_i^S < R_S$. Therefore, $R_{\text{all}}^{\text{fine}} - R'_{\text{all}} < 0$, indicating that the total resistance of the circuit has been optimized.

B.3 Analysis of Effectiveness of Chain-of-Self-consistency

Furthermore, we optimize the total circuit resistance from a different perspective, specifically by improving the resistance of validation resistor through self-consistency. In this approach, the validation resistor is decomposed into a parallel combination of multiple validation resistors and a meta-validation resistor with resistance R_{meta} , which verifies the correctness of the validation process. The original equation is thus reformulated as:

$$\begin{aligned} R_{\text{all}}^{\text{CoV}} &= R_0 + \frac{1}{\sum_{j=1}^k \sum_{i=1}^n \frac{1}{R_S}} + \sum_{j=1}^k (R_{\text{meta}}) + \frac{R_{\text{CoT}}}{n} \\ &= R_0 + \frac{R_S}{nk} + kR_{\text{meta}} + \frac{R_{\text{CoT}}}{n}. \end{aligned}$$

Clearly, as the sample size n and the meta-validation steps k increase, $\frac{R_S}{nk}$ decreases, leading to reduced difficulty in meta-validation. This significantly optimizes the total resistance and improves output power. Figure 6b illustrates this performance enhancement.

However, as the number of samples requiring validation grows, the model's accuracy first increases and then decreases. Specifically, for sufficiently large validation steps, the resistance satisfies:

$$\lim_{nk \rightarrow +\infty} R_{\text{all}}^{\text{CoV}} = R_0 + kR_{\text{meta}}. \quad (25)$$

With excessive validation steps, k becomes too large, resulting in $kR_{\text{meta}} > R_S$. Consequently, $R_{\text{all}}^{\text{CoV}}$ exceeds its optimized value, leading to a performance trend characterized by initial improvement followed by decline.

C Proof of Impact of Resistor Optimization

To compute the derivatives of P_{model} with respect to R_{CoT} , we start with the given expression:

$$P_{\text{model}} = \frac{(\mathcal{E}_{\text{model}} + \mathcal{E}_{\text{ICL}})^2 R_0}{(R_{\text{CoT}} + R_0)^2}. \quad (26)$$

According to Eq. 10, let $R_{\text{CoT}} = R_1 + R_2$, where $R_1 \gg R_2$, if R_1 is improved to $\frac{R_1}{k}$, the power can be calculated as:

$$P_{\text{model}}^1 = \frac{(\mathcal{E}_{\text{model}} + \mathcal{E}_{\text{ICL}})^2 R_0}{\left(\frac{R_1}{k} + R_2 + R_0\right)^2} \quad (27)$$

The corresponding power improvement is:

$$\Delta P_{\text{model}}^1 = P_{\text{model}}^1 - P_{\text{model}} \quad (28)$$

$$= \frac{(\mathcal{E}_{\text{model}} + \mathcal{E}_{\text{ICL}})^2 R_0}{(R_1 + R_2 + R_0)^2} - \frac{(\mathcal{E}_{\text{model}} + \mathcal{E}_{\text{ICL}})^2 R_0}{\left(\frac{R_1}{k} + R_2 + R_0\right)^2} \quad (29)$$

$$= (\mathcal{E}_{\text{model}} + \mathcal{E}_{\text{ICL}})^2 R_0 \left(\frac{1}{(R_1 + R_2 + R_0)^2} - \frac{1}{\left(\frac{R_1}{k} + R_2 + R_0\right)^2} \right) \quad (30)$$

Similarly, if R_2 is improved to the original $\frac{R_2}{k}$, the power improvement can be calculated as:

$$\Delta P_{\text{model}}^2 = (\mathcal{E}_{\text{model}} + \mathcal{E}_{\text{ICL}})^2 R_0 \left(\frac{1}{(R_1 + R_2 + R_0)^2} - \frac{1}{\left(R_1 + \frac{R_2}{k} + R_0\right)^2} \right) \quad (31)$$

To determine which improvement has a greater effect, consider:

$$\Delta P_{\text{model}}^1 - \Delta P_{\text{model}}^2 = (\mathcal{E}_{\text{model}} + \mathcal{E}_{\text{ICL}})^2 R_0 \left(\frac{1}{\left(\frac{R_1}{k} + R_2 + R_0\right)^2} - \frac{1}{\left(R_1 + \frac{R_2}{k} + R_0\right)^2} \right) \quad (32)$$

Define:

$$A = \frac{R_1}{k} + R_2 + R_0, \quad B = R_1 + \frac{R_2}{k} + R_0 \quad (33)$$

The fractional difference simplifies as:

$$\frac{1}{A^2} - \frac{1}{B^2} = \frac{B^2 - A^2}{A^2 B^2} \quad (34)$$

We need to prove that for $R_1 \gg R_2$ whether $B^2 - A^2$ larger or smaller than zero. Now, let's calculate $B^2 - A^2$:

$$B^2 - A^2 = (B - A)(B + A) \quad (35)$$

where:

$$B - A = \left(R_1 + \frac{R_2}{k} + R_0 \right) - \left(\frac{R_1}{k} + R_2 + R_0 \right) \quad (36)$$

$$= R_1 - \frac{R_1}{k} + \frac{R_2}{k} - R_2 \quad (37)$$

$$= R_1 \left(1 - \frac{1}{k} \right) + R_2 \left(\frac{1}{k} - 1 \right) \quad (38)$$

and:

$$B + A = \left(R_1 + \frac{R_2}{k} + R_0 \right) + \left(\frac{R_1}{k} + R_2 + R_0 \right) \quad (39)$$

$$= R_1 + \frac{R_1}{k} + R_2 + \frac{R_2}{k} + 2R_0 \quad (40)$$

Analysis of the Sign of $B^2 - A^2$:

$$B^2 - A^2 = (B - A)(B + A) \quad (41)$$

We only need to examine the sign of $B - A$, since $B + A > 0$ holds true at all times. since $R_1 \gg R_2$, and $1 - \frac{1}{k} > 0$ for $n > 1$, we have:

$$R_1 \left(1 - \frac{1}{k} \right) - R_2 \left(1 - \frac{1}{k} \right) > 0 \quad (42)$$

$$(R_1 - R_2) \left(1 - \frac{1}{k} \right) > 0 \quad (43)$$

$$B^2 - A^2 > 0 \quad (44)$$

$$\Delta P_{\text{model}}^1 - \Delta P_{\text{model}}^2 > 0 \quad (45)$$

Thus, $\Delta P_{\text{model}}^1 < \Delta P_{\text{model}}^2$ the difference is negative, and the proof is complete. Therefore, The greater the original difficulty of the task corresponding to the capability, the greater the impact on the final performance.